# Analysis and Estimation of the Probability of Failures in an Electric Lighting Network Using Mamdani Inference and Scaled Conjugate Gradient

**Mohammed Amine Jouahri**
**Zakaria Boulghasoul**
**Abdelouahed Tajer**
*Systems Engineering and Application Laboratory*
*Cady Ayyad University*
*Bd Abdelkrim Al Khattabi*
*Marrakech, 40000, Morocco*

This paper presents an intelligent fault detection system (FDS) for public lighting networks, designed to improve diagnostic accuracy and system reliability. The proposed system integrates the Mamdani fuzzy inference method and scaled conjugate gradient (SCG) neural networks to detect four key fault types: power, lighting, cloud cover sensor and road flow sensor. Inputs such as traffic flow, cloud cover, power supply and lighting intensity are used to ensure precise diagnostics. The Mamdani method offers strong interpretability and robustness in handling uncertainties, while the SCG algorithm enhances performance through efficient learning. Simulation results show fault detection probabilities exceeding 85%, confirming the effectiveness of the system. This paper demonstrates the potential of combining fuzzy logic and neural networks for reliable and intelligent monitoring of public lighting infrastructure.

*Keywords*: public lighting networks; fault detection; power faults; lighting faults; sensor faults; Mamdani inference; scaled conjugate gradient

## 1. Introduction

The optimization of energy consumption has become a global priority within the framework of energy transition and sustainable development [1]. Electrical lighting networks, due to their widespread use and significant contribution to energy demand, constitute a critical domain for improvement [2, 3]. However, these networks frequently encounter faults such as power fluctuations [4], electrical interruptions [5] and luminaire failures [6], leading to substantial energy losses and reduced overall system efficiency.

https://doi.org/10.25088/ComplexSystems.34.4.479

Accurate and rapid fault diagnosis is essential to minimize energy waste, reduce maintenance costs and ensure the optimal operation of lighting networks [7]. Conventional diagnostic methods involve visual inspections to identify physical anomalies [8, 9], electrical parameter measurements to detect imbalances [10, 11], lighting quality analysis to ensure compliance with standards [12, 13] and infrared thermography to identify thermal irregularities [14–16]. These practices are supplemented by technical tests such as continuity and insulation checks to prevent short circuits and major failures. While effective, these approaches are costly, time intensive and prone to human error. To address these limitations, integrating intelligent systems utilizing artificial intelligence (AI) techniques, such as fuzzy logic [17–19] and neural networks [20, 21], offers a promising alternative by automating diagnostics, enhancing accuracy and reducing operational costs.

AI is revolutionizing the diagnosis of public lighting networks [22] by enabling advanced capabilities for proactive fault detection [23], predictive maintenance [24] and energy optimization [25]. By analyzing real-time data from sensors monitoring parameters such as light intensity, energy consumption and environmental conditions, AI facilitates rapid anomaly detection and anticipates potential failures through trend analysis. Additionally, AI can adjust lighting levels based on actual needs, thereby reducing energy consumption while maintaining safety. By making these networks autonomous and adaptive, AI contributes to the development of sustainable, reliable and economically viable public lighting infrastructures.

In this paper, Section 2 presents the state of the art in electrical system diagnostics research. Section 3 describes in detail the methodology adopted to design the fault detection system (FDS). Section 4 outlines the development aspects of the FDS, using Mamdani's method and the scaled conjugate gradient (SCG) method. Section 5 proposes an experimental study, analyzing the results of MATLAB/Simulink simulations based on real data relating to road flow and cloud cover. Section 6 concludes by summarizing the results obtained and highlighting the advantages and limitations of each method.

## 2. Related Work

The diagnosis of electrical systems requires a series of visual examinations and functional tests to assess their integrity and performance. This process includes visual inspection to spot obvious damage, continuity tests to verify current flow, voltage tests to ensure voltage stability, grounding checks to avoid the risk of electrocution, thermographic analysis to identify hot spots, load tests to assess system

capacity, functional checks of electrical devices and analysis of the data collected to detect possible problems [26–28].

Integrating AI into electrical system diagnostics offers considerable advantages in terms of efficiency, accuracy and speed. AI algorithms can process large quantities of data from sensors installed on electrical equipment, as well as historical performance data. They can detect patterns, anomalies and trends that could indicate potential problems. Machine learning techniques enable these systems to continually improve their diagnostic capabilities by refining their ability to recognize new patterns [29–31].

Several studies have been carried out on the diagnosis and detection of faults in electrical systems.

In [32] a fuzzy logic–based method is developed for diagnosing direct current (DC) starter failures. This approach overcomes the uncertainties associated with models, noise and the stochastic behavior of variables and is capable of detecting six types of failure. This method is useful for quality control units as well as for maintenance and repair.

In [33] a method is proposed for detecting and classifying faults in medium-voltage direct current (MVDC) electrical systems. This method combines multiresolution wavelet transform analysis with artificial neural networks (ANNs). Simulations have demonstrated the effectiveness of this approach for detecting various types of faults.

In [34] a prototype is developed to collect data on various faults in a single-phase distribution network. Three machine learning algorithms—KNN, SVM and DT—were tested, with the DT model achieving 99.42% accuracy.

Research is conducted in [35] into the detection and localization of high-impedance faults in a distribution network. The study examines several algorithms, with SVM performing best for accurate detection and localization of these faults.

In [36] a new method is proposed for detecting and locating aging cable segments in underground distribution systems. The method is based on broadband transfer function measurement and the use of deep learning approaches, with experiments showing its effectiveness.

In [37] an integrated energy system (IES) is presented that uses machine learning technologies to improve fault detection in district heating systems in China. The IES-ML achieved 98.67% accuracy in fault detection.

More recently, [38] introduces an innovative electric drive system using a double-wound permanent magnet motor (DWPMM). This system aims to improve reliability while reducing costs. A fuzzy logic–based power switch open circuit fault diagnosis strategy has also been proposed, enabling faults, including intermittent faults, to be detected and located in real time.

https://doi.org/10.25088/ComplexSystems.34.4.479

This paper proposes an FDS for electrical lighting networks, based on Mamdani inference and the SCG algorithm. The system is designed to identify four types of faults: power, lighting, cloud cover sensor and traffic flow sensor.

A power fault is identified when the power supplied by the controller, which adjusts lighting based on traffic flow and cloud cover, is insufficient to meet lighting requirements. A lighting fault is detected in cases of nonfunctional luminaires despite adequate electrical power. A cloud cover sensor fault refers to an anomaly in the cloud coverage sensor, while a traffic flow sensor fault is identified when a malfunction disrupts traffic monitoring.

## 3. Problem Definition

The system presented in this paper is specifically designed to detect and locate faults within an electric lighting network. This advanced system is equipped to identify and distinguish between four distinct types of faults that may arise:

1. *Power*. This type of fault arises when the power supplied by the smart controller, which manages the electricity for the lighting network, is insufficient to meet the network's energy demands. The smart controller adjusts the power output based on changes in road traffic and cloud cover. A power fault is identified when the generated energy falls short of the requirements dictated by these two factors.
2. *Lighting*. This fault is detected when, despite sufficient energy production, lighting is absent. This indicates a failure separate from energy production, suggesting a problem in lighting distribution or activation.
3. *Cloud cover sensor*. This fault is identified when there is a significant difference between the actual value and the measured value of cloud cover, compromising lighting management.
4. *Road flow sensor*. This fault occurs when an inconsistency is observed between the actual road flow value and that measured by the sensor, reducing the effectiveness of traffic-based lighting adjustment.

To implement this fault detection and localization system, two AI approaches are adopted: fuzzy logic based on Mamdani's inference system (MIS), known for its ability to handle uncertain and imprecise data, and neural networks trained with the SCG algorithm, offering increased robustness and accuracy for modeling complex data.

System input parameters include road flow, cloud cover, electrical power generated by the smart controller and lighting network brightness, as well as the error between the actual value and the value detected by the cloud cover sensor, and the error between the actual value and the value detected by the road flow sensor. Based on these six inputs, the system is able to determine four types of fault. This

configuration enables a detailed and precise analysis of lighting network conditions, facilitating rapid and targeted intervention to correct identified faults.

## 4. Development of the Fault Detection and Location System

In this section, we design an FDS for electric lighting networks, using fuzzy logic (FL) based on Mamdani inference and neural networks trained with the SCG algorithm.

### 4.1 Fault Detection and Localization Using Fuzzy Logic Based on Mamdani's Inference System

The method developed in this section uses fuzzy logic with MIS to model the interactions between six input parameters and four types of output faults. Mamdani inference, one of the most popular fuzzy logic methods, relies on linguistic rules of the type If…Then… to model relationships between inputs and outputs. This process includes four main steps: fuzzification of inputs, evaluation of fuzzy rules, aggregation of outputs and defuzzification to produce a precise final value. This method is widely used in control and decision-making systems. Algorithm 1 is a summary of the essential steps in this process, from fuzzification of the input data to defuzzification to obtain a concrete output.

**Algorithm 1**. Mamdani fuzzy inference system (FIS).

**Require:** Input variables $x_1, x_2, \ldots, x_n$, fuzzy rules, membership functions for inputs and outputs, aggregation method, defuzzification method

**Ensure:** Defuzzified output $y$

1. **Fuzzification:**
2. **for** each input variable $x_i$ **do**
3. Compute membership degrees $\mu_i$ for all associated fuzzy sets
4. **end for**
5. **Rule Evaluation:**
6. **for** each fuzzy rule **do**
7. Compute condition degree using logical operators (e.g., min for AND, max for OR)
8. Apply condition degree to the rule's consequence (e.g., truncate output fuzzy set)
9. **end for**
10. **Aggregation:**
11. Combine all fuzzy rule outputs into a single fuzzy set using an aggregation method (e.g., max)

https://doi.org/10.25088/ComplexSystems.34.4.479

12. **Defuzzification:**
13. Convert the aggregated fuzzy set to a crisp output $y$ using a defuzzification method (e.g., centroid)
14. **return** $y$

Input parameters of the FDS include road flow, indicating traffic intensity; cloud cover, influencing available daylight; electrical power supplied by the controller to power the lighting network; and measured network brightness; as well as the error between the actual value and that detected by the cloud cover sensor, and the error between the actual value and that measured by the road flow sensor.

The system generates four outputs: the probability of power failure, indicating a risk of power supply failure; the probability of lighting failure, indicating a lack of light; the probability of cloud sensor failure; and the probability of road flow sensor failure. These outputs help to monitor and maintain optimal network operation by identifying and anticipating failures (see Figure 1).

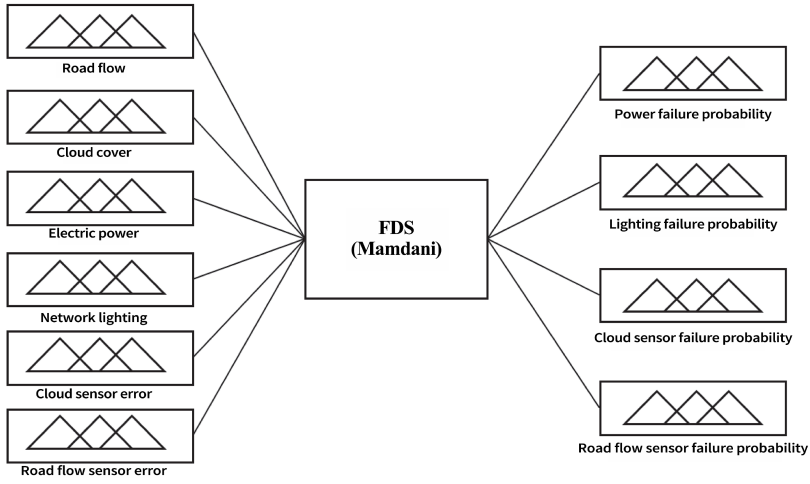


**Figure 1.** FDS data fusion algorithm structure.

In this paper, we detail the membership functions for the input and output parameters of the FDS, specifically choosing triangular membership functions. Figures 2 and 3 illustrate these membership functions for the input and output parameters of the FDS, respectively. Each parameter has been divided into three levels: low, medium and high. We consider the following input parameters:

- *Traffic flow*. The universe of discourse for this input ranges from 0 to 320 vehicles, reflecting traffic density, and is divided into three levels: low (0–100 vehicles), medium (50–250 vehicles) and high (200–320 vehicles).
- *Cloud cover*. The range of values for this input extends from 0% (clear sky) to 100% (complete cloud cover), with low (0–39%), medium (17–83%) and high (61–100%) levels.
- *Electrical power generated by the controller*. We have established that the lighting network is supplied with electrical power ranging from 0 to 30 kW, with low (0–10 kW), medium (5–25 kW) and high (20–30 kW) levels.
- *Network lighting*. Represented by the optical power emitted by the LEDs, this input covers a range from 0 W to 20 W, divided into low (0–8 W), medium (4–16 W) and high (12–20 W) levels.
- *Cloud sensor error*. The universe of discourse for this input ranges from −100% to 100%, with three defined levels: N (−100% to −20%), Z (−60% to 60%) and P (20% to 100%).
- *Road flow sensor error*. The universe of discourse for this input ranges from −320 to 320 and is divided into three levels: N (−320 to −64), Z (−200 to 200) and P (64 to 320).

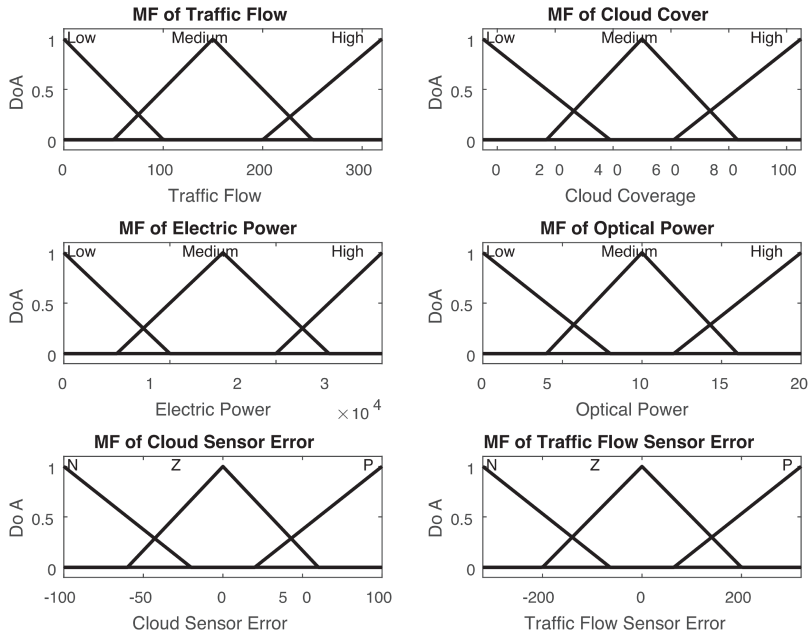


**Figure 2.** Input membership functions.

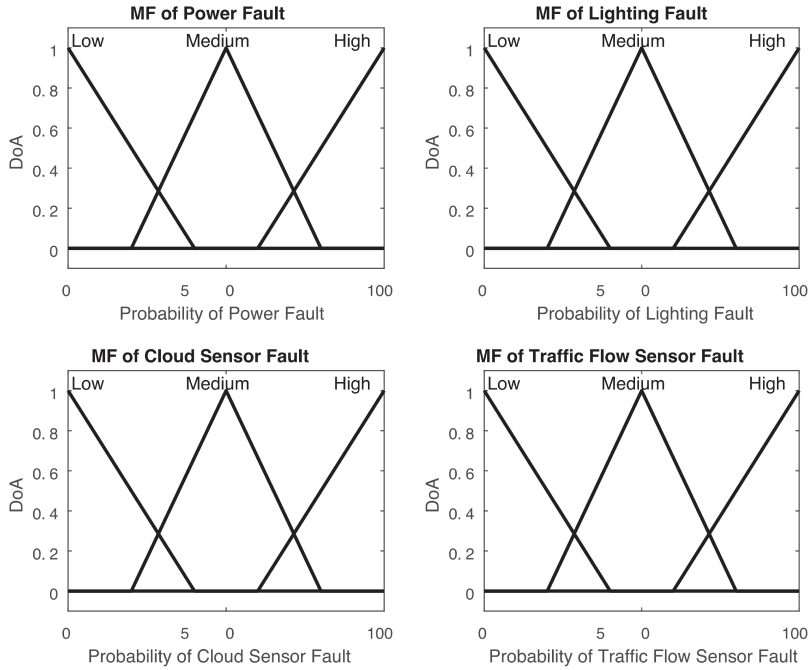


**Figure 3.** Output membership functions.

The system outputs are designed to identify four main types of faults:

- power
- lighting
- cloud sensor
- road flow sensor

For these four output parameters, the universe of discourse is defined between 0% and 100%, and each output is further divided into three levels: low (0–40%), medium (20–80%) and high (60–100%). This precise quantification of power and lighting fault levels enables rigorous assessment and effective management of anomalies detected in the electric lighting network. By structuring the universes of discourse and the levels of each parameter in this way, we facilitate a more detailed analysis and appropriate response to identified faults, guaranteeing better lighting system performance and reliability.

Tables 1 through 4 describe in detail the rules established for the FDS. Table 1 focuses on power faults, with a set of 27 rules covering all possible combinations of road flow, cloudiness and generated electrical power levels, enabling precise detection of power anomalies in the lighting network.

| | | Electric Power | | |
|---|---|---|---|---|
| Traffic Flow | Cloudiness | low | medium | high |
| low | low | low | medium | high |
| low | medium | medium | low | medium |
| low | high | medium | medium | low |
| medium | low | low | low | high |
| medium | medium | medium | low | high |
| medium | high | high | medium | low |
| high | low | medium | low | medium |
| high | medium | medium | high | low |
| high | high | high | high | low |

**Table 1.** Fuzzy rule base for power faults.

Table 2 contains six rules dedicated to lighting faults. They have been designed to identify variations in the light emitted by LEDs, as a function of the electrical power generated by the controller.

| | Brightness | | |
|---|---|---|---|
| Electric Power | low | medium | high |
| low | low | | |
| medium | medium | low | |
| high | high | medium | low |

**Table 2.** Fuzzy rule base for lighting faults.

Tables 3 and 4 show the rules for cloudiness and road flow sensor faults, respectively, each comprising three rules for detecting potential sensor malfunctions.

| Cloud Sensor Error | Cloud Sensor Fault |
|---|---|
| N | high |
| Z | low |
| P | high |

**Table 3.** Fuzzy rule base for cloud sensor faults.

| Traffic Flow Sensor Error | Traffic Flow Sensor Fault |
|---|---|
| N | high |
| Z | low |
| P | high |

**Table 4.** Fuzzy rule base for traffic flow sensor faults.

https://doi.org/10.25088/ComplexSystems.34.4.479

By combining these sets of rules, the system is able to monitor and analyze lighting network performance in depth, accurately detecting power, lighting and sensor faults and providing clear indications for their management and correction.

Having constructed the input and output functions, we tested the FDS using the surface viewer. Figure 4(a) shows this visualizer for the power supply fault. This graph reveals that, according to the rules defined in Table 1, the probability of a supply fault is high when road flow and cloud cover are high, but the electrical power generated is insufficient to meet lighting requirements. A power failure is also likely when road flow and cloud cover are low, but the electrical power generated is excessive, resulting in wasted energy.

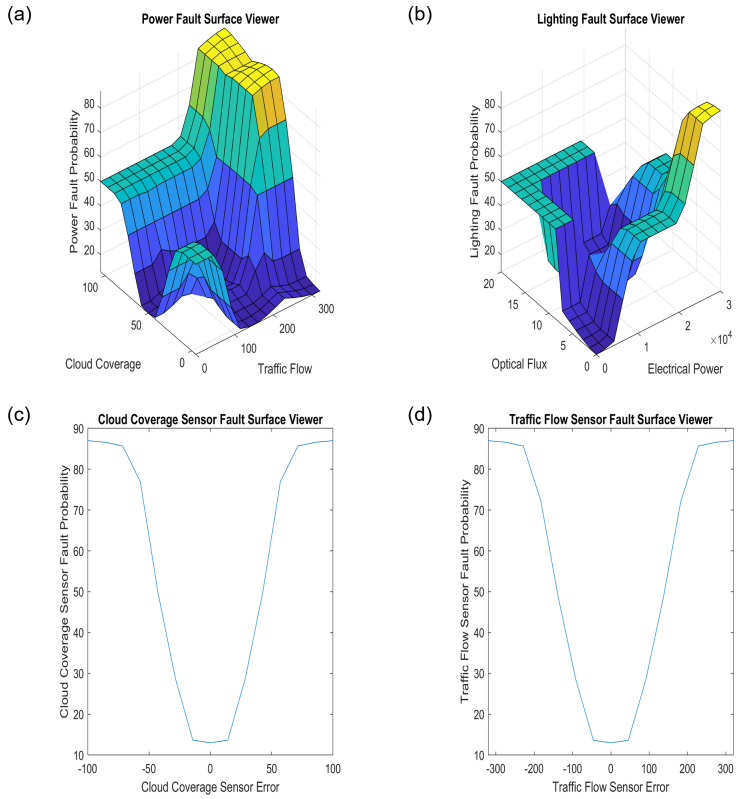


**Figure 4.** Surface viewer for: (a) power fault; (b) lighting fault; (c) cloud sensor fault; and (d) road flow sensor fault.

Figure 4(b) shows the surface viewer for lighting faults. According to this graph and the rules in Table 2, the probability of a lighting fault is high when lighting is insufficient, although the amount of electricity available to supply the network is adequate. This can occur

when, despite sufficient electrical power, the LEDs fail to reach the required lighting level, indicating a potential problem in the lighting system itself.

Figure 4(c) illustrates the surface viewer for cloud sensor faults. According to this graph and the rules in Table 3, the probability of a cloud sensor fault is high when there is a difference between the actual values and those captured by the sensor. This means, for example, that in cloudy weather, the sensor detects nothing, or vice versa.

Finally, Figure 4(d) shows the surface viewer for road flow sensor faults. Following the rules in Table 4, the probability of a road flow sensor fault is high when deviations are observed between the actual values and those captured by the sensor. This is particularly the case when there are vehicles on the road, but the sensor detects no road flow, or vice versa.

### 4.2 Analysis and Estimation of Failures in an Electric Lighting Network via Scaled Conjugate Gradient

The approach adopted in this case is based on the use of ANNs, in particular, the SCG algorithm. SCG is an extension of the classical conjugate gradient method, adapted specifically for training neural networks. Unlike standard gradient descent, which can suffer from slow convergence, SCG utilizes an approximation of the Hessian matrix (second-order derivatives) to dynamically adjust the search direction and step size. This allows SCG to converge faster while avoiding the computational cost of exact Newtonian methods. The algorithm begins with the initialization of weights and gradients, iteratively updating the weights along an optimized search direction. The inclusion of a scaling parameter $\sigma$ ensures numerical stability and prevents oscillations during updates. Due to these properties, SCG is particularly effective for training deep neural networks with complex cost functions. Algorithm 2 summarizes the essential steps of the SCG method for neural network training.

**Algorithm 2.** SCG.

**Require**: Cost function $E(w)$, gradient $\nabla E(w)$, initial weights $w_0$, scaling parameter $\sigma_0$, tolerance $\epsilon$, maximum iterations max_iter

**Ensure**: Optimized weights $w$, cost history

1. Initialize weights $w \to w_0$, gradient $g_0 \to \nabla E(w)$, search direction $d_0 \to -g_0$, iteration $k \to 0$
2. **while** $\|g_k\| > \epsilon$ and $k <$ max_iter **do**
3. Compute perturbation: $s_k \to \sigma_k \cdot d_k$
4. Approximate the Hessian: $v_k \to \frac{\nabla E(w+s_k)-\nabla E(w)}{\sigma_k}$
5. Update step size: $\alpha_k \to \frac{\|g_k\|^2}{d_k^\top v_k}$

6. Update weights: $w \rightarrow w + \alpha_k \cdot d_k$
7. Compute next gradient: $g_{k+1} \rightarrow \nabla E(w)$
8. Update search direction: $d_{k+1} \rightarrow -g_{k+1} + \frac{\|g_{k+1}\|^2}{\|g_k\|^2} \cdot d_k$
9. Adjust scaling parameter $\sigma_k$ if needed
10. Increment $k \rightarrow k + 1$
11. **end while**
12. **return** Optimized weights $w$, cost history

This methodological choice is in line with the previously developed fault detection system, which used Mamdani inference to identify anomalies. However, this new approach offers finer-grained modeling and enables complex relationships between different parameters to be captured.

The input parameters used in this system are identical to those previously employed in the FDS based on Mamdani inference. These include road flow, reflecting traffic intensity; cloud cover, which influences natural luminosity; electrical power generated by the controller; lighting network luminosity, a direct indicator of system performance; the error between the actual value and that detected by the cloud cover sensor; and the error between the actual value and that measured by the road flow sensor. From this data, the model generates four output parameters: the power fault probability, the lighting fault probability, the fault probability of the cloud cover sensors and the fault probability of the road flow sensors.

As part of this paper, we decided to develop two separate ANNs to handle faults identified in the public lighting network. This approach makes it possible to improve detection accuracy and robustness by specializing each artificial neural network (ANN) in the management of specific faults, depending on their characteristics and the nature of the parameters involved. The first network is designed to detect faults relating to power and lighting, since these faults have a direct impact on the quality of the illumination provided and require in-depth analysis of electrical values and luminosity. The second network is dedicated to faults in cloud cover and road flow sensors. These parameters, although different from the electrical ones, play a crucial role in adjusting lighting intensity according to weather and traffic conditions, which is essential for optimizing energy efficiency and road safety.

By dividing faults into two main categories and assigning each category a dedicated ANN, this approach reduces the complexity of each model while increasing the specificity of their predictions. This modular structure brings flexibility, facilitates network maintenance and enables better generalization and performance of the models.

### 4.2.1 Neural Network for Power and Lighting Fault Detection

The first neural network is primarily designed to detect faults in the network's power supply and lighting. It uses controller-generated power, brightness, road flow and cloud cover as input parameters, directly influencing power and lighting conditions. This network model comprises two hidden layers of 15 neurons each, with the activation functions logsig for the hidden layers and purelin for the output layer.

As previously mentioned, we opted for the SCG algorithm, using a learning rate of 0.05 and strict convergence criteria, with the aim of reducing overlearning and ensuring optimal generalization. Tests carried out on real data reveal high accuracy in detecting power and lighting faults. The performances obtained include an MSE of 2.1379 (Figure 5(a)); a correlation coefficient R of 0.99627 (Figure 5(b)), very close to 1; a gradient decreasing until reaching its minimum value of 2.7355 at iteration 1000 (Figure 5(c)); and an error varying

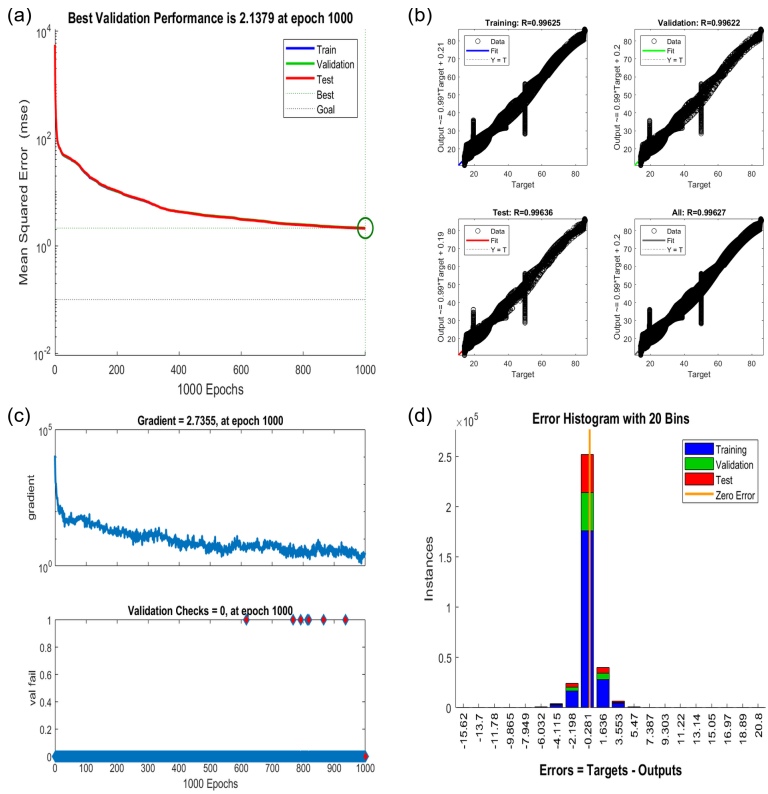


**Figure 5.** (a) Performance; (b) regression plot; (c) learning state; and (d) error histogram of the first ANN.

between −2.198 and 3.553 (Figure 5(d)). These results confirm the effectiveness of this architecture for defect detection.

### 4.2.2 Neural Network for Nebulosity and Road Flow Sensor Fault Detection

The second neural network is dedicated to the detection of faults affecting cloudiness and road flow sensors, key elements in ensuring the proper operation of the adaptive lighting system. Input parameters for this network include the reading errors associated with these sensors.

This network features a simple architecture, with a single hidden layer of 10 neurons. The logsig activation function is used for the hidden layer, while the output layer employs the purelin function. The SCG algorithm is also applied, with a learning rate of 0.05 to limit overlearning. The tests carried out demonstrate high efficiency in detecting sensor defects. The performances obtained include an MSE of 0.099887 (Figure 6(a)); a correlation coefficient R of 0.99983

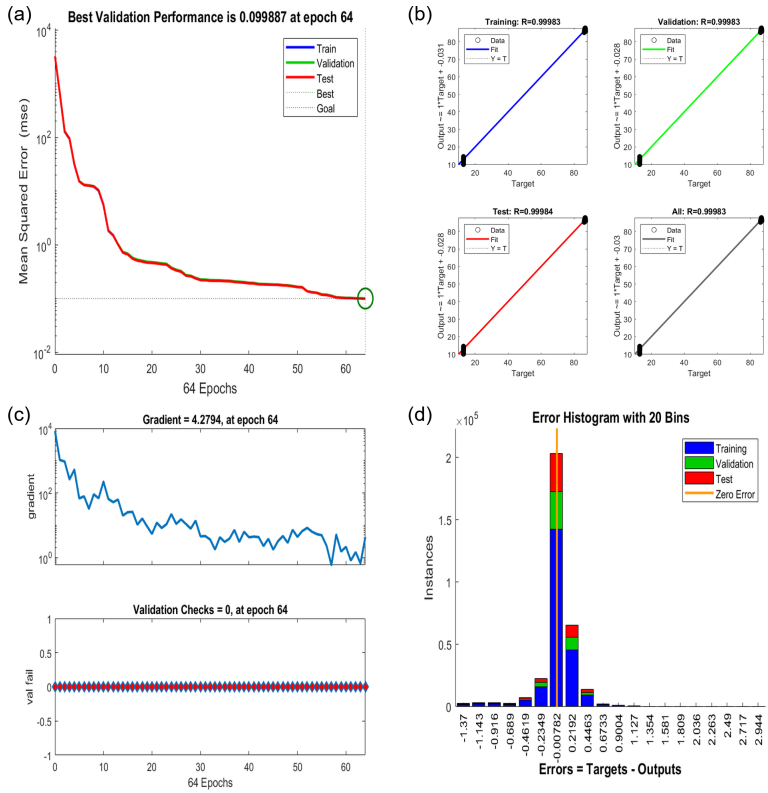


**Figure 6.** (a) Performance; (b) regression plot; (c) learning state; and (d) error histogram of the second ANN.

(Figure 6(b)), very close to 1; a gradient reaching a minimum value of 4.2794 at iteration 64 (Figure 6(c)); and an error varying between −0.4619 and 0.4463 (Figure 6(d)). These results confirm the reliability of this architecture for sensor fault detection.

## 5. Simulation Results and Discussion

After developing the FDS using the Mamdani inference method and SCG neural networks, we test it on the electric lighting network described and modeled in the previous sections. The block diagram of the fault detection system, applied to this lighting network, is shown in Figure 7.

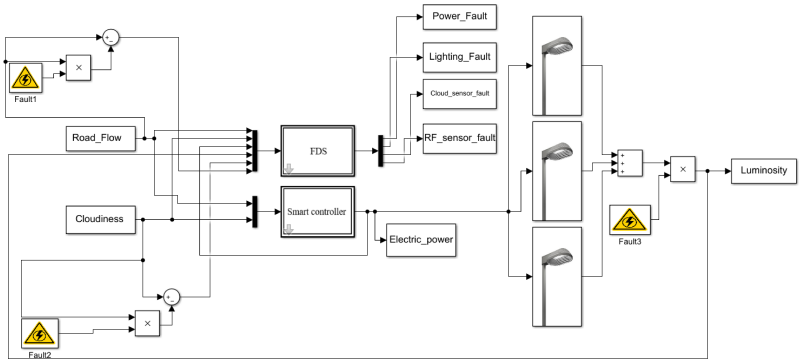


**Figure 7**. Block diagram of the FDS implemented on the electric lighting network.

The system operates as follows: To detect power failures, the system receives the electrical power generated by the intelligent controller. This controller dynamically adjusts the power according to variations in road flow and cloud cover. The system then compares the electrical power generated with the values for road flow and cloud cover. If road flow or cloud cover is high, but the electrical power generated is insufficient, the system signals a high probability of power failure. Conversely, if electrical power is high while road flow and cloud cover values are low, an anomaly is also suspected.

For lighting failure detection, the system analyzes the correspondence between the electrical energy supplied by the controller and the actual state of the lighting. If the controller generates an adequate amount of electrical energy, but the lighting is absent or defective, the system concludes that there is a high probability of a lighting failure. This detection process enables efficient monitoring and diagnosis of anomalies in the lighting network.

https://doi.org/10.25088/ComplexSystems.34.4.479

The system incorporates a methodological approach to detecting faults in the road flow and cloud cover sensors. With regard to the road flow sensor, the system compares the data captured by the sensor in real time with actual traffic observations or expected estimates, calculated from a historical database and current trends. For example, if the sensor indicates low traffic density when normal conditions predict dense traffic (such as rush hour), the system registers an inconsistency and detects a high probability of sensor failure. Furthermore, sudden and irregular variations in the values transmitted by the sensor that do not correspond to plausible traffic dynamics are also interpreted as malfunction signals.

For the cloud cover sensor, the system performs a similar analysis, comparing the data collected with external weather records or local predictive models. A prolonged absence of variation in cloud cover values, despite obvious changes in weather conditions (from clear to cloudy, for example), is a potential indicator of sensor failure. On the other hand, if the sensor registers high cloudiness in clear-sky conditions, or vice versa, the system identifies a discrepancy and concludes that the sensor is probably malfunctioning.

These analyses are enhanced by the use of sensor errors as input parameters to the intelligent model. The road flow sensor error is defined as the difference between the actual traffic density and the density measured by the sensor. Similarly, the cloud cover sensor error represents the difference between the actual cloud cover (obtained from reliable sources or standard references) and the measured cloud cover. When these errors exceed a predefined critical threshold, the system triggers an alert to signal a sensor fault.

The system will be evaluated in two separate tests, using real road flow and cloud cover data, to validate its effectiveness under practical conditions.

### 5.1 Test 1

The two signals shown in Figure 8 model the real-time variation in road flow and cloud cover, respectively, over a 24-hour period for the first test.

Figure 9 shows the various faults detected by the FDS in the lighting network over a continuous 24-hour period for the first test.

For this analysis, we have made the assumption that only faults with a probability exceeding 50% require immediate intervention for repair. This methodology aims to prioritize corrective actions and ensure optimized network maintenance.

Figure 9(a) illustrates a power fault. For the Mamdani method, this fault is detected between 08:33 and 09:39, with a probability exceeding the critical threshold of 50% and reaching a significant peak of

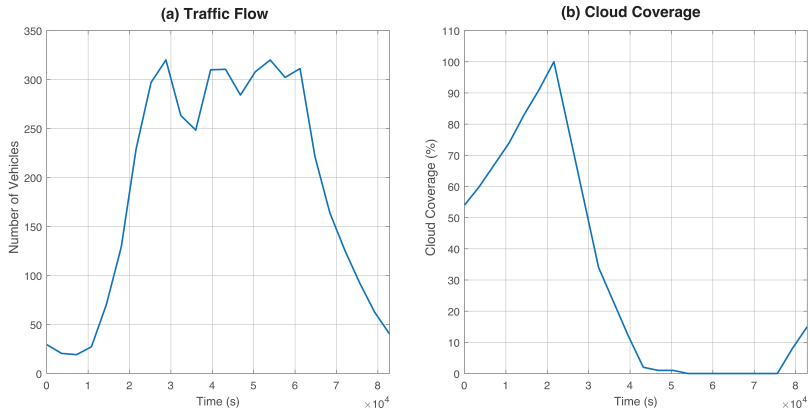


**Figure 8.** Real data for: (a) road flow; and (b) cloud cover (Test 1).

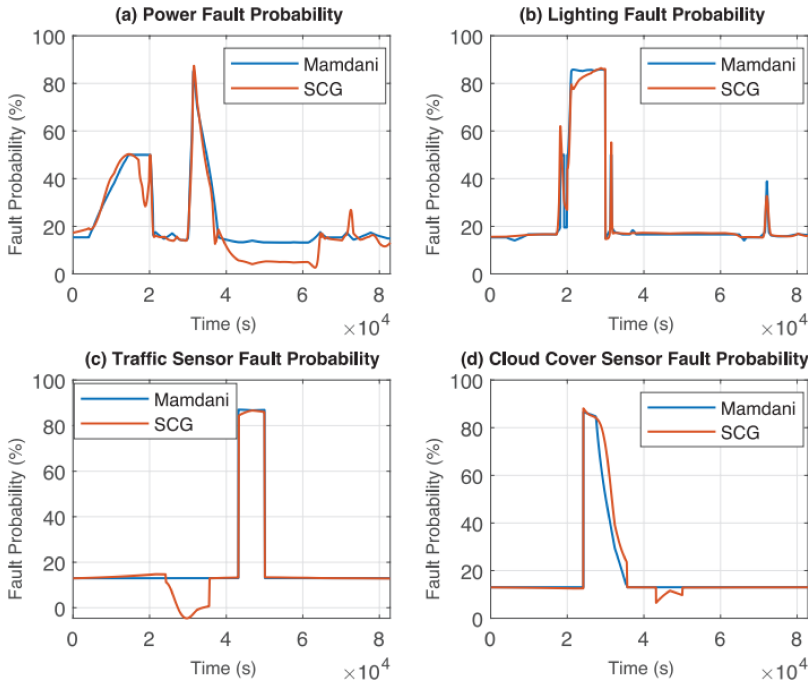


**Figure 9.** Fault probabilities for: (a) power; (b) lighting; (c) road flow sensor; and (d) cloud cover sensor (Test 1).

85.67% at 08:45. In parallel, for the SCG method, a power fault is identified over a slightly different period, between 08:36 and 09:31, with a probability peak of 87.37% observed at 08:46.

In Figure 9(b), a lighting fault was intentionally introduced between 05:33 and 08:19 to test the effectiveness of the FDS. The aim

of this experiment was to verify the system's ability to accurately identify this type of fault. The figure provides a detailed analysis of the probability of fault detection over the time interval concerned. The results show a progressive increase in the probability of detection, reaching a peak at 08:00 with a maximum value of 85.85% for the Mamdani method and 86.43% for the SCG method. This peak demonstrates that the system identified the fault with great accuracy at this precise moment, confirming the reliability and robustness of our detection methods under controlled conditions.

Similarly, Figure 9(c) illustrates the results obtained following the deliberate introduction of a fault in the road flow sensor, which occurred between 12:00 and 13:52. The aim of this experiment was to assess the detection system's ability to detect this specific type of anomaly. Analysis of the data shown in the figure reveals a progressive increase in the probability of fault detection throughout the time interval under consideration. This probability reaches a first notable peak of 86.99% at 12:00 for the Mamdani method, followed by a second peak of 86.61% at 13:00 for the SCG method.

Finally, Figure 9(d) shows the results obtained after the intentional introduction of a fault in the cloud cover sensor, simulated between 06:43 and 09:52. The aim of this experiment was to test the detection system's ability to identify this type of anomaly, which can disrupt input parameters critical to the optimal operation of the lighting network. Analysis of the data reveals a significant increase in the probability of fault detection throughout the simulated time interval. The Mamdani method registers an initial probability peak of 86.49% right at the start of the interval, at 06:43, while the SCG method reaches an even higher peak of 88.09% at the same time. These results highlight the accuracy and effectiveness of both approaches in identifying faults associated with environmental sensors. This ability to detect faults quickly and reliably ensures better proactive management and targeted maintenance of the public lighting network.

Tables 5 through 8 provide further details on the origin of the various faults detected by the FDS.

| | Peak of Fault | Time (h) | Road Flow | Cloud (%) | EP (kW) |
|---|---|---|---|---|---|
| Mamdani | 85.67% | 08:45 | 276.9 | 39.29 | 18.59 |
| SCG | 87.37% | 08:46 | 276.2 | 39.01 | 18.21 |

**Table 5.** Detailed overview of power fault origin.

Table 5 gives details of the origin of the power fault identified by the FDS. As previously indicated, the probability of fault detection reaches 85.67% at 8:45 with the Mamdani method and 87.37% at

8:46 with the SCG method. At this point, road flow is 276, which is considered high, while cloud cover is 39%, a value close to the median. At the same time, the electrical power supplied by the controller feeding the lighting network is 18 kW. These observations suggest that the fault detected is probably linked to insufficient electrical power to meet the needs of the lighting network, particularly in view of the heavy traffic. This highlights the need for an adequate power supply to ensure optimal operation of the lighting network, particularly during periods of heavy traffic.

Table 6 details the origin of the lighting fault. It reveals that at 08:00, the absence of lighting is associated with zero optical power (0 W), despite the fact that the network provides a power supply of 26.71 kW. This situation led to a progressive increase in the probability of failure, reaching a maximum of 85.85% with the Mamdani method and 86.43% with the SCG method. These results point to a malfunction in the conversion or transmission of electrical energy to the lighting system, suggesting a potential failure of the latter, despite an adequate power supply.

| | Peak of Fault | Time (h) | Electric Power (kW) | Optic Power (W) |
|---|---|---|---|---|
| Mamdani | 85.85% | 08:00 | 26.71 | 0 |
| SCG | 86.43% | 08:00 | 26.71 | 0 |

**Table 6.** Detailed overview of lighting fault origin.

Table 7 shows the origin of the road flow sensor fault. As shown in the table, the fault reaches its maximum value of 86.99% at 12:00 for the Mamdani method, and 86.61% at 13:00 for the SCG method. At 12:00, the actual road flow value for the Mamdani method is 310.5, while the value detected by the sensor is −4.65, a negative value that seems inconsistent. For the SCG method, at 13:00, the actual road flow value is 284.3, but the sensor detects a value of 2.5, showing that it has not captured the correct road flow value. This indicates an anomaly in the road flow sensor.

| | Peak of Fault | Time (h) | Road Flow | Detected Value |
|---|---|---|---|---|
| Mamdani | 86.99% | 12:00 | 310.5 | −4.65 |
| SCG | 86.61% | 13:00 | 284.3 | 2.5 |

**Table 7.** Detailed overview of traffic sensor fault origin.

Finally, Table 8 shows the origin of the cloud cover sensor fault. As shown, the fault reaches its maximum value at 06:43, with 86.49% for the Mamdani method and 88.09% for the SCG method.

At this time, the actual cloud cover value is 84.11%, while the value detected by the sensor is 4.2%, indicating that the sensor has not detected the correct value, suggesting an anomaly in the cloud cover sensor.

| | Peak of Fault | Time (h) | Cloud (%) | Detected Value |
|---|---|---|---|---|
| Mamdani | 86.49% | 06:43 | 84.11 | 4.2 |
| SCG | 88.09% | 06:43 | 84.11 | 4.2 |

**Table 8.** Detailed overview of cloud cover sensor fault origin.

## 5.2 Test 2

The two signals shown in Figure 10 model the real-time variation in road flow and cloud cover, respectively, over a 24-hour period for the second test.

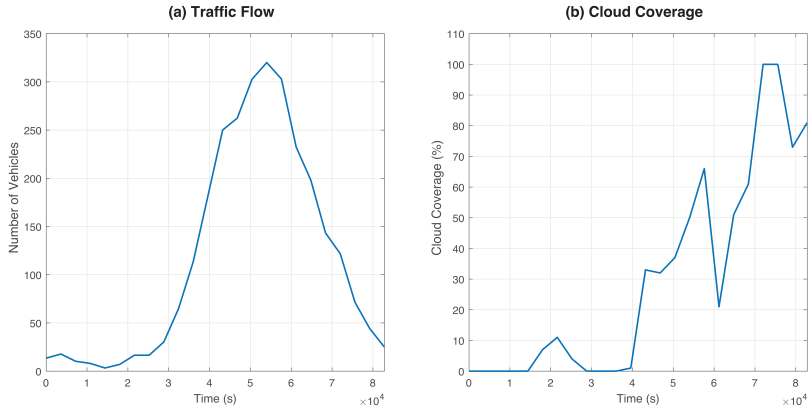


**Figure 10.** Real data for: (a) road flow; and (b) cloud cover (Test 2).

Figure 11 illustrates the various faults detected by the detection system within the lighting network over a continuous 24-hour period as part of the second test. In accordance with the defined criteria, only faults with a probability greater than 50% are considered to require intervention.

In this second test, Figure 11(a) highlights the detection of two power faults by the system developed. The first fault was identified between 11:48 and 14:30, with a peak probability of 85.62% at 14:09 according to the Mamdani method and a peak of 77.76% at 13:56 for the SCG method. The second fault was detected between 16:22 and 16:52, reaching a peak of 85.19% at 16:29 using the Mamdani method and a peak of 74.28% at 16:39 using the SCG method.

Figure 11(b) illustrates the results obtained following the intentional introduction of a lighting fault between 13:52 and 16:22, as

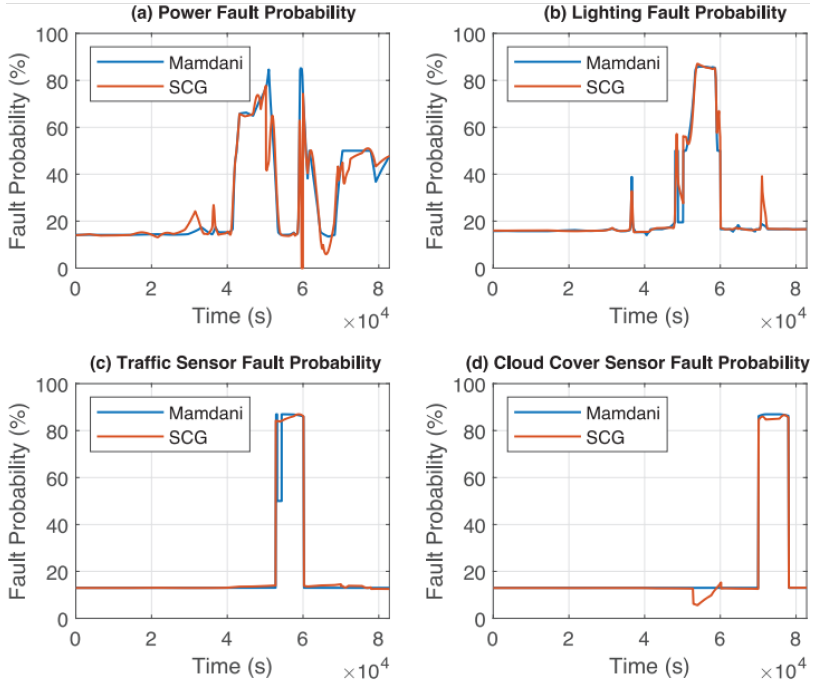


**Figure 11.** Fault probabilities for: (a) power; (b) lighting; (c) road flow sensor; and (d) cloud cover sensor (Test 2).

part of the second test. As with the first test, the purpose of this maneuver was to evaluate the efficiency and accuracy of the FDS developed. The data shows a progressive increase in the probability of detection throughout the defined time interval. The system reached a probability peak at 15:09, with a maximum value of 85.83% for the Mamdani method, and at 15:00, with a probability of 87.07% for the SCG method.

Figure 11(c) shows the results obtained after the deliberate introduction of a fault in the road flow sensor, simulated to occur between 14:39 and 16:43. The aim of this experiment was to assess the detection system's ability to accurately identify this type of malfunction under realistic conditions. Analysis of the data shown in the figure reveals a progressive increase in the probability of fault detection over the specified time interval. For the Mamdani method, the probability reaches a significant peak of 87% at 15:06, indicating effective fault identification at that precise moment. For the SCG method, the maximum peak recorded was 86.99% at 16:20, also confirming the high performance of the system in this context.

Finally, Figure 11(d) illustrates the results obtained following the deliberate introduction of a simulated fault in the cloud cover sensor, which occurred between 19:26 and 21:39. The aim of the simulation

was to assess the system's ability to accurately detect this type of malfunction under controlled conditions. Analysis of the data revealed a significant increase in the probability of fault detection over the simulated time interval. For the Mamdani method, a first notable peak is recorded at 20:00 with a probability of 86.99%, confirming rapid and effective detection. For its part, the SCG method shows a slightly shifted maximum peak at 21:21, reaching a probability of 86.65%.

As with the first test, Tables 9 through 13 provide further details on the origin of the various faults detected by the system during the second test.

Tables 9 and 10 detail the origin of the two power supply faults identified by the detection system. For the first fault, the probability of detection reaches 84.62% at 14:09 with the Mamdani method and 77.76% at 13:56 with the SCG method. At these times, road flow is high (305.4 for Mamdani and 300.5 for SCG), while cloud cover is moderate (39% for Mamdani and 36.72% for SCG). At the same time, the electrical power supplied by the controller to the lighting network is 20 kW. For the second fault, the probability of detection is 85.19% at 16:29 for the Mamdani method and 74.28% at 16:36 for the SCG method. Road flow remains high (286.1 for Mamdani and 256 for SCG) and cloud cover is average (43.75% for Mamdani and 36% for SCG), while the electrical power supplied is 19.32 kW for the Mamdani method and 15.13 kW for the SCG method. These observations suggest that the faults detected are probably due to insufficient electrical power to meet the needs of the lighting network, particularly during periods of heavy traffic. This underscores the importance of an adequate power supply to guarantee the network's smooth operation, particularly during heavy traffic hours.

| | Peak of Fault | Time (h) | Road Flow | Cloud (%) | EP (kW) |
|---|---|---|---|---|---|
| Mamdani | 84.62% | 14:09 | 305.4 | 39 | 20 |
| SCG | 77.76% | 13:56 | 300.5 | 36.72 | 20 |

**Table 9.** Detailed overview of the first power fault origin.

| | Peak of Fault | Time (h) | Road Flow | Cloud (%) | EP (kW) |
|---|---|---|---|---|---|
| Mamdani | 85.19% | 16:29 | 268.1 | 43.75 | 19.32 |
| SCG | 74.28% | 16:36 | 256 | 36 | 15.13 |

**Table 10.** Detailed overview of the second power fault origin.

Table 11 shows the origin of the lighting failure in the second test. According to the data, the fault peaks at 85.83% at 15:09 using the Mamdani method and at 87.07% at 15:00 using the SCG method. At

these times, the controller delivers an electrical power of 26 kW, while the optical power emitted by the lighting network is zero (0 W). These observations reveal a malfunction in the conversion or transmission of electrical energy to the lighting system, suggesting a possible failure of the latter, despite a sufficient power supply.

| | Peak of Fault | Time (h) | Electric Power (kW) | Optic Power (W) |
|---|---|---|---|---|
| Mamdani | 85.83% | 15:09 | 26.67 | 0 |
| SCG | 87.07% | 15:00 | 26.47 | 0 |

**Table 11.** Detailed overview of lighting fault origin.

Table 12 details the origin of the road flow sensor failure in the second test. The fault peaks at 87% at 15:06 with the Mamdani method and 86.99% at 16:20 with the SCG method. At 15:06, for the Mamdani method, the actual road flow value is 315.9, while the sensor detects an inconsistent value of −4.06, a negative measurement. Similarly, for the SCG method, at 16:20, the actual road flow value is 278.4, but the sensor reads 6.07, showing an inability to correctly capture the actual flow, revealing an anomaly in the road flow sensor.

| | Peak of Fault | Time (h) | Road Flow | Detected Value |
|---|---|---|---|---|
| Mamdani | 87% | 15:06 | 315.9 | −4.06 |
| SCG | 86.99% | 16:20 | 278.4 | 6.07 |

**Table 12.** Detailed overview of traffic sensor fault origin.

Table 13 illustrates the failure of the cloud cover sensor. The fault peaks at 20:00 with 86.99% for the Mamdani method and at 21:21 with 86.65% for the SCG method. At these times, actual cloud cover is high (100% for Mamdani and 90.39% for SCG), but the sensor reports very low values (0.7% for Mamdani and 1.22% for SCG), indicating an inability to detect cloud cover correctly and confirming a fault in the sensor.

| | Peak of Fault | Time (h) | Cloud (%) | Detected Value |
|---|---|---|---|---|
| Mamdani | 86.99% | 20:00 | 100 | 0.7 |
| SCG | 86.65% | 21:21 | 90.39 | 1.22 |

**Table 13.** Detailed overview of cloud cover sensor fault origin.

https://doi.org/10.25088/ComplexSystems.34.4.479

## 6. Conclusion

The aim of this paper was to design an intelligent system capable of detecting and locating faults in an electric lighting network, based on two distinct approaches: a fuzzy logic system based on Mamdani inference and the scaled conjugate gradient (SCG) backpropagation method. The system uses key input parameters, such as road flow and cloud cover, to identify and diagnose various types of failure, including power and lighting failures, as well as those related to road flow and cloud cover sensors. A quantitative performance evaluation of the two approaches highlighted their respective efficiencies in different fault detection scenarios.

The Mamdani method stood out for its high accuracy, particularly for power and lighting faults. In the first test, it achieved maximum detection rates of 85.67% for power failures and 85.85% for lighting failures, while maintaining stable performance in both tests. For the road flow and cloud cover sensor faults, the maximum values achieved were 86.99% and 86.49%, respectively, slightly below the peak of 88.09% obtained by the SCG method for the cloud cover sensor fault in the first test. Despite these discrepancies, the Mamdani method demonstrated consistent accuracy and reliability, making it ideal for applications requiring consistency and early fault detection.

The SCG method, on the other hand, showed superior performance for peak detection of certain defects. It achieved a detection probability of 88.09% for the cloud cover sensor fault in the first test, outperforming the Mamdani method by 1.6%, and a detection of up to 87.07% for the lighting fault in the second test, 1.24% ahead of the Mamdani method. On the other hand, the SCG method was slightly more effective at detecting power failures early, although its detection peaks were lower (77.76% vs. 84.62% for the first power failure in the second test and 74.28% vs. 85.19% for the second power failure in the same test). In addition, the SCG method showed a faster convergence rate, requiring fewer iterations to train the neural network. This is particularly advantageous for real-time applications where rapid response is crucial.

Both methods demonstrated that they could detect defects with relatively high accuracy, but both had certain limitations. The Mamdani method, although reliable, showed slightly lower detection peaks for defects in road flow and cloud cover sensors, while the SCG method showed greater sensitivity to noise and overfitting in dynamic environments, which could affect its performance in real-world conditions.

In conclusion, both methods are highly effective for fault detection in LED street lighting systems. The Mamdani method offers high consistency and reliable performance, particularly for power supply faults, while the SCG method offers faster convergence and superior

detection for lighting faults as well as faults in road flow and cloud cover sensors. Future work could explore hybrid models that combine the strengths of both methods, improving the robustness and adaptability of fault detection systems in intelligent street lighting applications. This research lays the foundation for more advanced artificial intelligence–driven infrastructure management solutions, with the potential for greater fault detection accuracy, early fault diagnosis and increased operational efficiency.

## References

[1] A. A. Bazmi and G. Zahedi, "Sustainable Energy Systems: Role of Optimization Modeling Techniques in Power Generation and Supply—A Review," *Renewable and Sustainable Energy Reviews*, **15**(8), 2011 pp. 3480–3500. doi:10.1016/j.rser.2011.05.003.

[2] A. Ozadowicz and J. Grela, "Energy Saving in the Street Lighting Control System—A New Approach Based on the EN-15232 Standard," *Energy Efficiency*, **10**(3), 2017 pp. 563–576. doi:10.1007/s12053-016-9476-1.

[3] Y. Jiang, Y. Shuai, X. He, X. Wen and L. Lou, "An Energy-Efficient Street Lighting Approach Based on Traffic Parameters Measured by Wireless Sensing Technology," *IEEE Sensors Journal*, **21**(17), 2021 pp. 19134–19143. doi:10.1109/JSEN.2021.3089208.

[4] I. Azcarate, J. J. Gutierrez, A. Lazkano, P. Saiz, K. Redondo and L. A. Leturiondo, "Towards Limiting the Sensitivity of Energy-Efficient Lighting to Voltage Fluctuations," *Renewable and Sustainable Energy Reviews*, **59**, 2016 pp. 1384–1395. doi:10.1016/j.rser.2016.01.022.

[5] I. Tristiu, M. Eremia, C. Bulac and L. Toma, "Multi-criteria Reconfiguration of Distribution Electrical Networks for Minimization of Power Losses and Damage Cost Due to Power Supply Interruption," in *2007 IEEE Lausanne Power Tech*, Lusanne, Switzerland, Piscataway, NJ: IEEE, 2007 pp. 385–390. doi:10.1109/PCT.2007.4538348.

[6] T. Smialkowski and A. Czyzewski, "Detection of Anomalies in the Operation of a Road Lighting System Based on Data from Smart Electricity Meters," *Energies*, **15**(24), 2022 9438. doi:10.3390/en15249438.

[7] M. Kowsalya, S. A. A. Rajasree, B. Kalaimathi, G. Amrish, R. Dhinesh and S. Divakar, "Smart Streetlight Fault Detection and Location Tracking System," in *2024 4th International Conference on Sustainable Expert Systems (ICSES)*, Kaski, Nepal, Piscataway, NJ: IEEE, 2024 pp. 1263–1267. doi:10.1109/ICSES63445.2024.10762956.

[8] F. Lopes, P. Rocha and A. Coelho, "Towards Automated Visual Inspection of Electrical Grid Assets for the Smart Grid—An Application to HV Insulators," in *2024 IEEE International Conference on Smart Grid Communications (SmartGridComm)*, Oslo, Norway, Piscataway, NJ: IEEE, 2024 pp. 347–352. doi:10.1109/SmartGridComm60555.2024.10738034.

[9] F. Zhou, G. Wen, Y. Ma, H. Geng, R. Huang, L. Pei, W. Yu, L Chu and R. Qiu, "A Comprehensive Survey for Deep-Learning-Based Abnormality Detection in Smart Grids with Multimodal Image Data," *Applied Sciences*, **12**(11), 2022 5336. doi:10.3390/app12115336.

[10] S. Z. Malik, A. H. Khawaja, A. K. Janjua and M. Kazim, "A Contactless Method for Unbalanced Loading Detection in Power Distribution Lines by Magnetic Measurements," *IEEE Transactions on Instrumentation and Measurement*, **69**(10), 2020 pp. 7472–7483. doi:10.1109/TIM.2020.2983339.

[11] M. Irhoumah, R. Pusca, E. Lefevre, D. Mercier and R. Rromary, "Evaluation of the Voltage Supply Unbalance and Detection of the Short-Circuit Faults in Induction Machine through the Neighboring Magnetic Field," in *2021 International Conference on Applied and Theoretical Electricity (ICATE)*, Craiova, Romania, Piscataway, NJ: IEEE, 2021 pp. 1–6. doi:10.1109/ICATE49685.2021.9465061.

[12] P. R. Boyce, H. M. Brandston and C. Cuttle, "Indoor Lighting Standards and Their Role in Lighting Practice," *Lighting Research & Technology*, **54**(7), 2022 pp. 730–744. doi:10.1177/14771535221126413.

[13] N. Cincar, A. Simovic and Z. Sehovac, "Lighting of Workspaces in Compliance with Standards," in *2024 IEEE Third International Conference on Power Electronics, Intelligent Control and Energy Systems (ICPEICES)*, Delhi, India, Piscataway, NJ: IEEE, 2024 pp. 868–872. doi:10.1109/ICPEICES62430.2024.10719300.

[14] A. S. N. Huda and S. Taib, "Application of Infrared Thermography for Predictive/Preventive Maintenance of Thermal Defect in Electrical Equipment," *Applied Thermal Engineering*, **61**(2), 2013 pp. 220–227. doi:10.1016/j.applthermaleng.2013.07.028.

[15] M. S. Jadin and S. Taib, "Recent Progress in Diagnosing the Reliability of Electrical Equipment by Using Infrared Thermography," *Infrared Physics & Technology*, **55**(4), 2012 236–245. doi:10.1016/j.infrared.2012.03.002.

[16] Y. L. dit Leksir, M. Mansour and A. Moussaoui, "Localization of Thermal Anomalies in Electrical Equipment Using Infrared Thermography and Support Vector Machine," *Infrared Physics & Technology*, **89**, 2018 pp. 120–128. doi:10.1016/j.infrared.2017.12.015.

[17] H.-C. Chin, "Fault Section Diagnosis of Power System Using Fuzzy Logic," *IEEE Transactions on Power Systems*, **18**(1), 2003 pp. 245–250. doi:10.1109/TPWRS.2002.807095.

[18] R. Perez, E. Inga, A. Aguila, C. Vásquez, L. Lima, A. Viloria and M.-A. Henry, "Fault Diagnosis on Electrical Distribution Systems Based on Fuzzy Logic," in *Advances in Swarm Intelligence: 9th International Conference, ICSI 2018*, Shanghai, China, Proceedings, Part II 9 (Y. Tan, Y. Shi and Q. Tang, eds.), Cham: Springer, 2018 pp. 174–185. doi:10.1007/978-3-319-93818-9_17.

[19] W. Chen and A. M. Bazzi, "Logic-Based Methods for Intelligent Fault Diagnosis and Recovery in Power Electronics," *IEEE Transactions on Power Electronics*, **32**(7), 2017 pp. 5573–5589. doi:10.1109/TPEL.2016.2606435.

[20] S. Duer, K. Zajkowski, M. Harnicárová, H. Charun and D. Bernatowicz, "Examination of Multivalent Diagnoses Developed by a Diagnostic Program with an Artificial Neural Network for Devices in the Electric Hybrid Power Supply System 'House on Water'," *Energies*, **14**(8) 2021 2153. doi:10.3390/en14082153.

[21] W. Chine, A. Mellit, V. Lughi, A. Malek, G. Sulligoi and A. M. Pavan, "A Novel Fault Diagnosis Technique for Photovoltaic Systems Based on Artificial Neural Networks," *Renewable Energy*, **90**, 2016 pp. 501–512. doi:10.1016/j.renene.2016.01.036.

[22] D. Tang, F. Ding, B. Deng, P. Zhang, Q. Wang and H. Lv, "An Intelligent Fault Diagnosis Method for Street Lamps, in *2021 International Conference on Internet, Education and Information Technology (IEIT 2021)*, Suzhou, China, Piscataway, NJ: IEEE, 2021 pp. 300–303. doi:10.1109/IEIT53597.2021.00073.

[23] R. P. S. Kumar and R. Vadivel, "IOT Based Smart Street Light Fault Detection Management System," *World Journal of Advanced Research and Reviews*, **21**(3), 2024 pp. 1659–1666. doi:10.30574/wjarr.2024.21.3.0685.

[24] D. Carneiro, D. Nunes and C. Sousa, "A Decision-Support System for Preventive Maintenance in Street Lighting Networks," in *Hybrid Intelligent Systems: 18th International Conference on Hybrid Intelligent Systems (HIS 2018)*, Porto, Portugal (A. M. Madureira, A. Abraham, N. Gandhi and M. L. Varela, eds.), Cham: Springer, 2020 pp. 272–281. doi:10.1007/978-3-030-14347-3_26.

[25] R. Carli, M. Dotoli and R. Pellegrino, "A Decision-Making Tool for Energy Efficiency Optimization of Street Lighting," *Computers & Operations Research*, **96**, 2018 pp. 223–235. doi:10.1016/j.cor.2017.11.016.

[26] J. Sun, S.-Y. Qin, and Y.-H. Song, "Fault Diagnosis of Electric Power Systems Based on Fuzzy Petri Nets," *IEEE Transactions on Power Systems*, **19**(4), 2004 pp. 2053–2059. doi:10.1109/TPWRS.2004.836256.

[27] H. Henao, G.-A. Capolino, M. Fernandez-Cabanas, F. Filippetti, C. Bruzzese, E. Strangas, R. Pusca, et al., "Trends in Fault Diagnosis for Electrical Machines: A Review of Diagnostic Techniques," *IEEE Industrial Electronics Magazine*, **8**(2), 2014 pp. 31–42. doi:10.1109/MIE.2013.2287651.

[28] C. M. Furse, M. Kafal, R. Razzaghi and Y.-J. Shin, "Fault Diagnosis for Electrical Systems and Power Networks: A Review," *IEEE Sensors Journal*, **21**(2), 2021 pp. 888–906. doi:10.1109/JSEN.2020.2987321.

[29] W. G. Fenton, T. M. McGinnity and L. P. Maguire, "Fault Diagnosis of Electronic Systems Using Intelligent Techniques: A Review," *IEEE Transactions on Systems, Man, and Cybernetics, Part C (Applications and Reviews)*, **31**(3), 2001 pp. 269–281. doi:10.1109/5326.971655.

[30] Y. L. Murphey, M. A. Masrur, Z. Chen and B. Zhang, "Model-Based Fault Diagnosis in Electric Drives Using Machine Learning," *IEEE/ASME Transactions On Mechatronics*, **11**(3), 2006 pp. 290–303. doi:10.1109/TMECH.2006.875568.

[31] E. Chai, P. Zeng, S. Ma, H. Xing and B. Zhao, "Artificial Intelligence Approaches to Fault Diagnosis in Power Grids: A Review," in *2019 Chinese Control Conference (CCC)*, Guangzhou, China, Piscataway, NJ: IEEE, 2019 pp. 7346–7353. doi:10.23919/ChiCC.2019.8865533.

[32] O. Bay and R. Bayir, "A Fault Diagnosis of Engine Starting System via Starter Motors Using Fuzzy Logic Algorithm," *Gazi University Journal of Science*, **24**(3), 2011 pp. 437–449. dergipark.org.tr/tr/download/article-file/83182.

[33] W. Li, A. Monti and F. Ponci, "Fault Detection and Classification in Medium Voltage DC Shipboard Power Systems with Wavelets and Artificial Neural Networks," *IEEE Transactions on Instrumentation and Measurement*, **63**(11), 2014 pp. 2651–2665. doi:10.1109/TIM.2014.2313035.

[34] R. A. Sowah, N. A. Dzabeng, A. R. Ofoli, A. Acakpovi, K. M. Koumadi, J. Ocrah and D. Martin, "Design of Power Distribution Network Fault Data Collector for Fault Detection, Location and Classification Using Machine Learning," in *2018 IEEE 7th International Conference on Adaptive Science & Technology (ICAST)*, Accra, Ghana, Piscataway, NJ: IEEE, 2018 pp. 1–8. doi:10.1109/ICASTECH.2018.8506774.

[35] M. Sarwar, F. Mehmood, M. Abid, A. Q. Khan, S. T. Gul and A. S. Khan, "High Impedance Fault Detection and Isolation in Power Distribution Networks Using Support Vector Machines," *Journal of King Saud University-Engineering Sciences*, **32**(8), 2020 pp. 524–535. doi:10.1016/j.jksues.2019.07.001.

[36] Y. Wu, P. Zhang and G. Lu, "Detection and Location of Aged Cable Segment in Underground Power Distribution System Using Deep Learning Approach," *IEEE Transactions on Industrial Informatics*, **17**(11), 2021 pp. 7379–7389. doi:10.1109/TII.2021.3056993.

[37] P. Wang, P. Poovendran and K. B. Manokaran, "Fault Detection and Control in Integrated Energy System Using Machine Learning," *Sustainable Energy Technologies and Assessments*, **47**, 2021 101366. doi:10.1016/j.seta.2021.101366.

[38] K. Wang, X. Jiang, S. Wang and Z. Han, "Power Switch Open Circuit Fault Diagnosis Strategy for Novel Fault-Tolerant Electric Drive System Based on Fuzzy Logic," *Energy Reports*, **8**(13), 2022 pp. 914–921. doi:10.1016/j.egyr.2022.08.149.